DOI: 10.23968/2500-0055-2023-8-2-33-48

CALCULATION AND TESTING OF A REINFORCED CONICAL BRIDGE BEAM

Assylkhan Jalairov[1], Dauren Kumar[2]*, Nurzhan Dosaev[3], Gulzhan Nuruldaeva[4], Khaini-Kamal Kassymkanova[4], Gulshat Murzalina[4]

[1]Department of Transport Construction, Bridges and Tunnels, International University of Transportation and Humanities, Almaty, Republic of Kazakhstan

[2]Department of Cartography and Geoinformatics, Al-Farabi Kazakh National University, Almaty, Republic of Kazakhstan

[3]Department of Science and Introduction of New Technologies, National Center for Quality of Road Assets, Astana, Republic of Kazakhstan

[4]Satbayev University, Almaty, Republic of Kazakhstan

*Corresponding author's e-mail: daurendkb@gmail.com

Abstract

Introduction: The paper addresses the compliance of the actual strength and deformation properties of the standard precast block (hereinafter — UPB 185.25) with the design data. **Purpose of the study**: We aimed to check convergence of the experimental data for a reinforced concrete beam with variable outline of the bottom chord with the design assumptions. **Methods:** In the course of the study, the moments of inertia at each section of the unit were taken averaged, in steps. Each section was calculated separately. The results were then summed up. In addition, the calculated values were verified using the finite element method in MIDAS. **Results:** The adopted design assumptions based on the test results showed high convergence of the results and confirmed the compliance of the beam in terms of stiffness, crack resistance, and strength. The control crack opening width a_{cr} = 0.2 mm was achieved at a load of 503.2 kg, which is 22.7 % higher than the design load.

Keywords: beam deflection, control loads, crack resistance, graph-analytic method, UPB 185, FEM analysis.

Introduction

Beams of variable cross-section, characterized by variable geometric and physical parameters, have a number of particular features as compared to beams of constant cross-section. Specifically, reinforced concrete bridge beams ensure the architectural expressiveness of the assembled superstructure, are characterized by lower weight, and involve bench assembly in the manufacture of units without prestressed reinforcement. The latter makes it possible to simplify the manufacturing technology due to the lack of special channels for the use of high-strength reinforcement ropes, and the injection of specially selected solutions for grouting these channels. Processes for anchoring high-strength reinforcement ropes with subsequent prestressing of bridge beams were discussed, in particular, in papers by Jalairov et al. (2022a, 2022b). Besides, the joints of beams of variable cross-section require high-quality filling with cast-in-situ concrete, ensuring tight jointing and adhesion of cast-in-situ and precast concrete.

The design of beams of variable cross-section was earlier studied by Timoshenko (1965), Smirnov (1961), and Ruditsyn — using the method of breaking loads (Ruditsyn, 1940).

The variety of shapes and sections of such heterogenous beams poses the problem of determining their characteristics by various methods. For instance, in the works of the Russian researchers Gusev and Saurin (2017, 2018), the vibrations of heterogeneous beams and variational approaches to finding the eigen frequencies of such beams were described in detail following the analysis of publications based on materials from foreign press. The classical variational formulations, the method of integro-differential relations, energy estimates of the quality of the solution, a family of variational formulations, and a connection with classical variational principles were presented. It was shown that the proposed two-sided quality criteria for an approximate solution make it possible to obtain high-precision solutions for mathematical models of conventional concrete beams of small size.

The minimization of the weight of thin curved beams, the stress state of which is described by the Saint–Venant theory, was considered by Petukhov (1980). The effect of the cross-sectional shape on

the stress state was studied. It was assumed that each point of the beam must satisfy some condition for the strength of the material, and the optimal design of the conical beams must satisfy the critical load in bending (Wang et al., 1986). The cantilever and hinged beams were considered under the action of a uniformly distributed and concentrated load. The solution to the problem was achieved by two independent approaches: 1) using the energy method of Timoshenko; 2) using the Lagrange multiplier and the gradient expression of the problem.

Balduzzi et al. (2016) presented equations of compatibility, equilibrium and governing equations, including those for conical beams. It was shown that the shear distribution depends not only on the resultant vertical stress but also on the horizontal resultant stress and bending moment. The complex geometry of non-prismatic beams leads to the fact that each generalized deformation depends on all generalized stresses, in contrast to prismatic beams.

The spline method for the numerical calculation of the natural vibration frequency of a beam with a variable cross-section was also discussed by researchers (Cazzani et al., 2016; Zhernakov et al., 2017). The second order of convergence makes it possible to increase the calculation accuracy with almost six significant digits for the first ten forms of natural frequencies of beams with an exponentially changing width of a rectangular section.

Barham and Idris (2021) described the large increment method for the nonlinear analysis of Timoshenko beam structures. The essence of the method is to separate the linear equations of global equilibrium and compatibility from local nonlinear equations. This makes it possible to reduce errors in the step-by-step solution of nonlinear structural problems, which is typical for the finite element method (FEM). The final Timoshenko beam version formulated for solving beam structures with a rectangular and wide flange section, based on two numerical examples, showed a more accurate result with less computational algorithms.

A solution of Timoshenko–Ehrenfest beam problems using the theory of functional connections was given by Yassopoulos et al. (2021). This method is an alternative one, and under certain boundary conditions, in comparison with the finite element method, the design prerequisites of the theory of functional relationships may not work. But when solving some problems, the application of the theory of functional relationships allows you to quickly solve differential equations in comparison with FEM.

An analytical solution for the flat behavior of conical monosymmetric I-beams was considered by Chockalingam et al. (2020, 2021). An analytical formulation of the Timoshenko beam was proposed, which included the relationship of axial bending in basic differential equations. This approach allows us to consider a cone-shaped I-beam with a monosymmetric section as a straight line segment along the central line of the wall. This solution can be used within the FEM to design an accurate one-dimensional tapered beam element.

An analysis of the shear characteristics of a reinforced concrete conical beam with corrugated steel inclusions in the wall was presented by Zhou et al. (2019a, 2019b, 2021). It was shown that in conical beams, the lateral force near the supports is perceived not only by trapezoidal corrugated steel walls, as in the case of prismatic beams, but also by reinforced concrete walls. These theoretical assumptions are confirmed with experimental results and FEM calculations.

Zhong et al. (2021) presented an experimental and numerical analysis of crack propagation in reinforced concrete structures on a three-phase concrete model. In reinforced concrete structures, including conical beams, the Weibull distribution model can be used to describe microcracks in concrete. To study the behavior of cracks in the structure, a numerical program written in the parametric design language ANSYS and the tool control language was used. The simulation results showed good agreement with the experimental data.

Tayfur et al. (2021) presented an approach to determining the crack resistance of non-prismatic reinforced concrete beams based on the elastic and plastic behavior of reinforced concrete under static load. Two non-prismatic beams with hinged supports were tested with the construction of the deformation diagrams of reinforced concrete.

Resan and Zamel (2021a, 2021b) provided results of bending tests involving models of T-shaped reinforced concrete beams. As a way of control, the behavior of a prismatic beam was analyzed. The T-shaped beams differed in the height of the ribs in the longitudinal direction at the ends and middle of the beam, as well as the ribs in the transverse direction. The results generally confirm the effectiveness of T-beams in terms of material consumption with a single concrete strength and percentage of reinforcement.

From the analysis of the above sources, it follows that a significant number of works cover various methods for finding the modes and frequencies of vibrations of non-prismatic beams. There are also laboratory studies to clarify the strength and deformation characteristics and the process of cracking of such beams. However, there is very little information on the testing of full-scale reinforced concrete beams and their simplified calculation. In this paper, as an object of research, the results of tests of a conical reinforced concrete bridge beam and the beam calculation according to the standards of the Republic of Kazakhstan are considered.

The research was aimed at identifying the compliance of the calculated positions of the beam by the method of strength of materials and finite elements of the real operation of the beam under load.

The novelty of the research presented in this paper consists in proving the convergence of the design and experimental data in the calculation of the variable section of the beam with ledges, assuming an elastic stage of behavior.

Materials and Methods

Preparation for beam testing

Fig. 1 shows the front and cross-sections of the UPB 185.25 unit at its ends. The unit height in the support area is 2087 mm, and at the opposite end — 515 mm. The unit length is 18.5 m. Table 1 presents data on the dimensions of the UPB 185.25 unit along its length. The unit reinforcement with rods was earlier considered by Shalkarov et al. (2018).

The compressive strength class of concrete in the UPB 185.25 unit was taken as B35. The volume of concrete in the beam was 8.77 m^3. The concrete unit was at the age of 54 days as of the time of testing.

Rods with a diameter of 32 and 36 mm, class A400 (A-III), grade 25Mn2Si in accordance with GOST 5781-82 (SP RK 3.03-112-2013) were used as main longitudinal reinforcement in the upper and lower chords of the unit. In the support area of the unit, bends were installed from rebars with a diameter of 28 mm, class A400 (A-III), grade 25Mn2Si in accordance with GOST 5781-82. Reinforcement consumption in the beam was

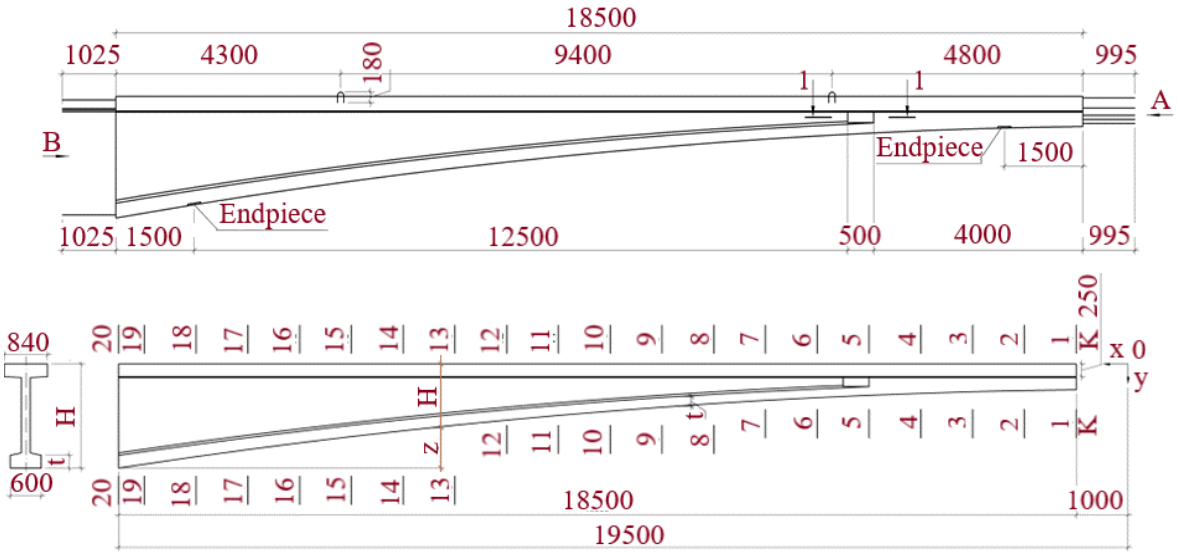

H = 0.507+0.003952(x+1)x, m; z = 2.087 – H, m; t = 0.138+0.006x, m.

(a) Front

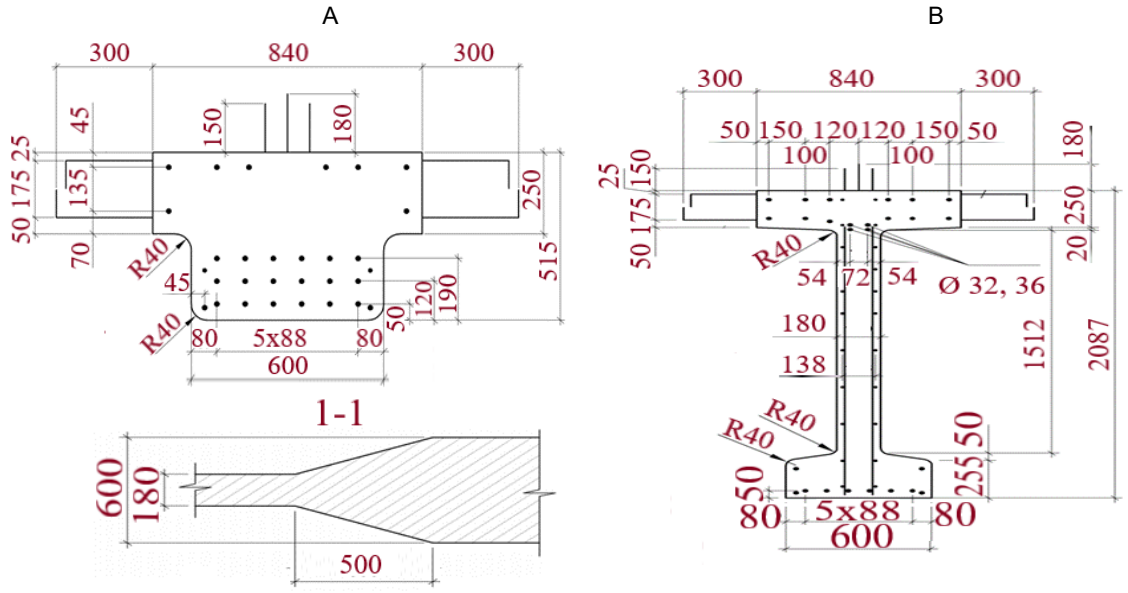

Fig. 1. Front and cross-sections of the UPB 185.25 unit

Table 1. **Data on the dimensions of the UPB 185.25 unit along its length**

Section No.	20	19	18	17	16	15	14	13	12	11	10	9	8	7	6	5	4	3	2	1	0
x, mm	19,500	19,000	18,000	17,000	16,000	15,000	14,000	13,000	12,000	11,000	10,000	9000	8000	7000	6000	5000	4000	3000	2000	1000	0
H, mm	2087	2009	1859	1716	1582	1455	1337	1226	1123	1029	942	863	791	728	643	626	586	554	531	515	507
z, mm	0	78	228	371	505	632	750	861	964	1058	1145	1224	1296	1359	1414	1461	1501	1553	1556	1572	1580
t, mm	255	252	246	240	234	228	222	216	210	204	198	192	186	180	174	168					

as follows: class A-III — 563 kg/m^3, class A-I — 8.6 kg/m^3. The weight of the embedded parts was 142.5 kg, and the total weight of the beam, taking into account the reinforcement, was 25.15 t.

As a rule, the diagrams of bending moments show that their greatest values can be found in the places where the blocks are joined together on intermediate supports and in the middle of the middle span structures (Smirnov, 1961). Accordingly, in the sections of the UPB 185.25 unit, between sections 20-20 and 19-19 and between sections 2-2 and 1-1 (see Fig. 2), a diagram of bending moments with different signs should be obtained in tests. Control loading tests are recommended to be carried out according to the schemes provided in the design documentation. Table 2 shows the geometric characteristics of the beam.

The creation of such a test scheme would require the development of a special power bench and significant tangible costs. In this regard, by

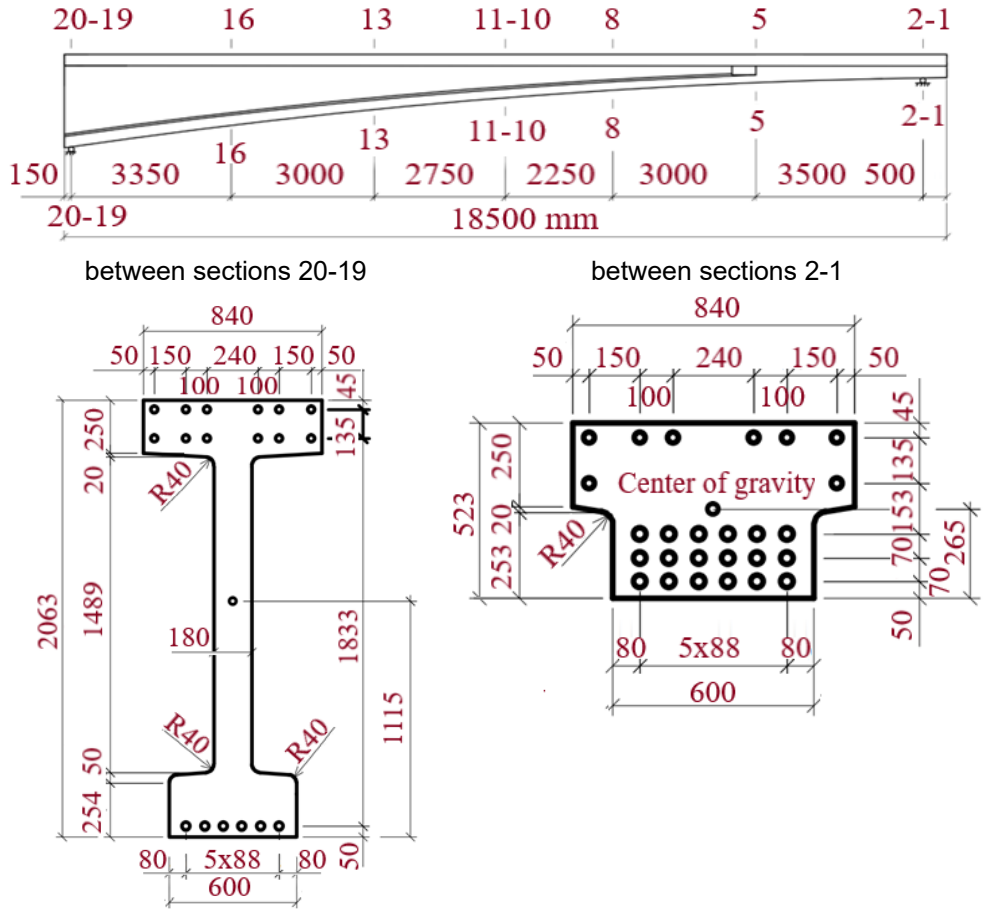

Fig. 2. Diagram of the UPB 185.25 unit, cross-sections and geometric characteristics of the unit

agreement with the design organization, another test scheme for the unit was adopted, which also makes it possible to assess its operational reliability. The process of preparing the unit for testing is shown in Fig. 3a.

The design model of the unit adopted for testing represented a freely supported single-span beam loaded in the middle of the span with a concentrated force P. In accordance with this design model, control loads were also determined in terms of strength, stiffness and crack resistance (see Fig. 3b).

To create and control the load when testing the UPB 185.25 unit, a power installation was used, which included two hydraulic jacks with a load capacity of 500 kN each, a pressure gauge, high-pressure hoses, and an electric pumping station.

The design length of the UPB 185.25 prototype was 17.85 m, and the axes of the supporting parts were located at a distance of 0.15 m from the elevated end of the unit, and 0.5 m from the lowered end. The test scheme of the UPB 185.25 unit corresponded to the design diagram shown in Fig. 2. Fig. 3c shows mechanical devices — deflectometers installed on the unit, which had a scale division of 0.1 mm, and the deflectometers under load P, which had a scale division of 0.01 mm. The test took into account the weight of the loading devices, which was 5.65 kN.

To load the unit, a power bench design was developed, which made it possible to transfer the load to the test specimen. As a counterweight, an anchor was made of cast-in-situ reinforced concrete with its anchoring in rocky ground. The length and number of the anchors embedded in rocky ground were selected in such a way that they could withstand the maximum load created by two hydraulic jacks.

During the tests, the deflections of the unit in the considered middle section under the jacks were determined, at a distance of 2.75 m and 2.25 m in each direction from the considered section and at a distance of 3.35 m and 3.50 m from the axes of the unit support. The settlement of the supports was also monitored using dial indicators with a scale division of 0.01 mm. Crack opening was determined using a Brinell microscope with a scale of 0.05 mm (Fig. 3c).

The load was applied to the unit in stages. After each stage of loading, readings were taken from deflectometers and indicators. Based on the test results, the stiffness, crack resistance and strength of the experimental structure were evaluated. The process of preparing the unit for testing is shown in Fig. 3a.

According to Table 40 of Regulations SP RK 3.03-112-2013 (Committee for Construction, Housing and Communal Services and Land Management of the Ministry of National Economy of the Republic of Kazakhstan, 2015), the category of crack resistance requirements for the UPB 185.25 unit is 3c, allowing cracking under the action of standard loads.

Control load for strength, crack resistance and stiffness testing

Control load for strength testing

The control load for strength testing is determined in accordance with the provisions set out in SP RK 3.03-112-2013 and GOST 8829-94 (Gosstroy of Russia, 1998).

Hereinafter, the calculations of the geometric characteristics and the calculated values are omitted, and only the resulting values are given.

The test load P_{test} is taken to be 682 kN.

According to clause B.1 of Appendix B (GOST 8829-94), the value of the control load Pc for testing the strength of the UPB 185.25 unit is determined by multiplying the value of the test load P_{test} corresponding to the bearing capacity of the unit, determined by calculation taking into account the design resistance of concrete and reinforcement and the adopted loading diagram in Fig. 4, by the safety factor C.

The value of the safety factor C for the 1st case of failure along the normal section due to reaching the yield point in longitudinal tensile reinforcement is determined according to Table B.1 of Appendix B (GOST 8829-94). For A400 class reinforcement, the safety factor C is assumed to be C = 1.3. Taking into account the adopted safety factor, the control breaking strength load is taken equal to:

$$P_k = C \cdot P_{test} = 1{,}3 \cdot 682 = 887 \text{ kN}. \quad (1)$$

Control load for crack resistance testing

According to Table 40 of Regulations SP RK 3.03-112-2013, in beams with non-tensioned reinforcement to which the category of crack resistance requirements 3c applies, under the action of standard loads, crack opening normal to the longitudinal axis of the element with a width of up to 0.3 mm is allowed. Taking into account the safety factor C = 0.7 and the correction factor (Section B.12 of SP RK 3.03-112-2013), the revised control crack opening width is taken to be a_{cr} = 0.2 mm.

In the Technical Regulations of the Republic of Kazakhstan “Safety requirements for buildings and structures, building materials and products” (Government of the Republic of Kazakhstan, 2010),

Table 2. **Geometric characteristics of the beam**

Cross-sectional area, A_{red}	7415.1 · 10^2 cm^2
Distance from the bottom of the unit to the center of gravity of the section, U_{bot}	1115 cm
Inertia moment of the section, I_{red}	43,118,818 · 10^4 cm^4

(a) the process of preparing the unit for testing

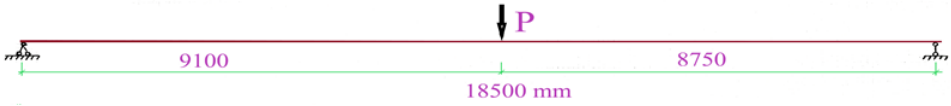

(b) design test scheme

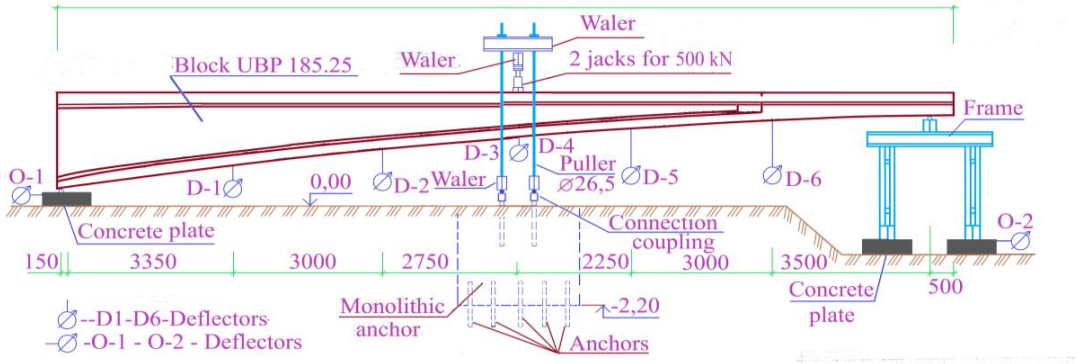

(c) power bench for the placement of mechanical devices

Fig. 3. Test scheme of the UPB 185.25 unit

it is noted that building structures can be designed and manufactured according to other regulatory documents, provided that their requirements are not lower than the requirements specified in the regulatory documents of the national level. The calculation of the control load for crack resistance testing is carried out according to the Regulations of the Russian Federation (SP 63.13330.2018 “Concrete and reinforced concrete structures”), in which the crack opening width is limited to 0.3 mm as in SP RK 3.03-112-2013.

The control load for crack resistance testing according to the calculation is taken equal to P_c = 410 kN at the control crack opening width a_{cr} = 0.2 mm.

Control load for stiffness testing

The control load for stiffness testing of the UPB 185.25 unit is determined from the condition for assessing the state of the unit at the moment preceding the crack formation in the lower fiber of the concrete unit and is taken equal to P_c = 178 kN.

To determine the control deflection of the UPB 185.25 unit in the middle of its span from the action of the control load P_c = 178 kN, we use the graph-analytical method (Smirnov, 1961), which makes it possible to determine displacements in beams of variable cross-section, assuming that at this stage of testing, the unit behaves practically in elastic stages.

Fig. 4a shows a design diagram of the unit loaded with the concentrated force P, which in our case is a control load for stiffness. In Fig. 4b, a diagram of bending moments M is shown, where in the considered sections 2 ÷ 6 their values are given in general form from the action of the control load for stiffness.

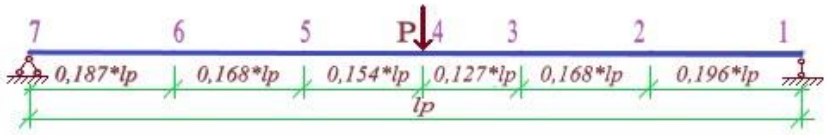

a) unit loaded with the concentrated force P

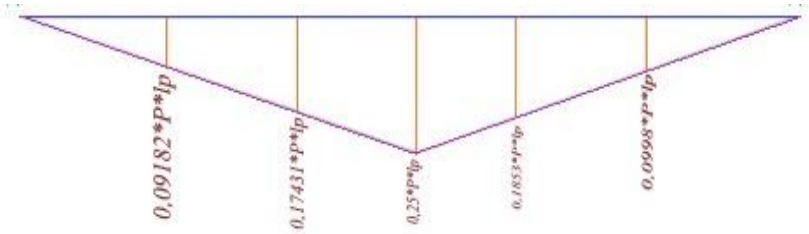

b) bending moments M

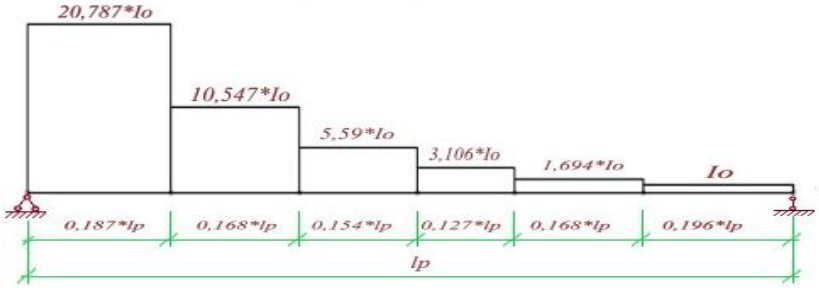

c) the averaged values of the moments of inertia in unit sections 2-3, 3-4, 4-5, 5-6, and 6-7 in fractions of the value I_0

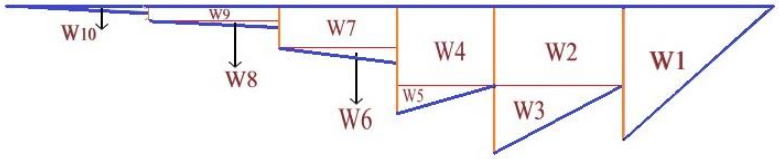

d) separate areas in the center of gravity of which weights W_i are applied

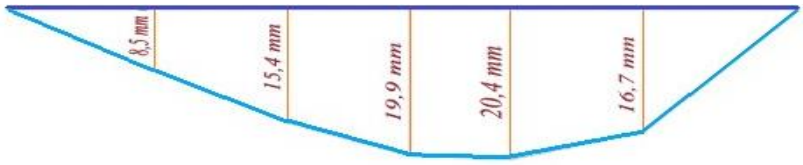

e) the effect of fictitious loads W_i

Fig. 4. Determining the deflection of the beam

Since the stiffness of the unit along its length changes according to a curvilinear law, in this case, to simplify the calculation, the moments of inertia at each section of the unit are taken averaged, in steps. We take the averaged moment of inertia I0 of the unit section 1-2 as a basis. Fig. 4c shows the averaged values of the moments of inertia in unit sections 2-3, 3-4, 4-5, 5-6, and 6-7 in fractions of the value I_0.

The fictitious load shown in Fig. 4d changes abruptly along the unit length. This is due to the fact that the unit stiffness values are different at each of the sections, therefore, after dividing the values from the diagram of bending moments M by different stiffness values, we can obtain their own fictitious loads. Naturally, it is difficult to determine fictitious moments from such a complex load. The fictitious load shown in Fig. 4d is replaced by a lumped fictitious weight system, as shown in Fig. 4d.

Such a replacement consists in the fact that the diagram shown in Fig. 4d is divided into separate areas, in the center of gravity of which weights Wi are applied (see Fig. 4d), which are numerically equal to the corresponding areas of the diagram.

It should be borne in mind that when determining the elastic modulus of concrete, reduction factors are introduced that take into account the heat and moisture treatment of concrete (k_1 = 0.9) and the elastic-plastic properties of concrete under a short-

term action of the load P during the unit loading (k_2 = 0.85).

Fig. 4e shows the effect of fictitious loads Wi, determined taking into account the above-mentioned reduction factors k_1 and k_2. The values of the fictitious loads W_i, according to the calculation, are taken as follows:

$$W_1 = 0.00978 \cdot \frac{P \cdot l_p^2}{E_b \cdot I_0}; \quad (2)$$

$$W_2 = 0.00990 \cdot \frac{P \cdot l_p^2}{E_b \cdot I_0}; \quad (3)$$

$$W_3 = 0.00424 \cdot \frac{P \cdot l_p^2}{E_b \cdot I_0}; \quad (4)$$

$$W_4 = 0.00758 \cdot \frac{P \cdot l_p^2}{E_b \cdot I_0}; \quad (5)$$

$$W_5 = 0.00132 \cdot \frac{P \cdot l_p^2}{E_b \cdot I_0}; \quad (6)$$

$$W_6 = 0.00104 \cdot \frac{P \cdot l_p^2}{E_b \cdot I_0}; \quad (7)$$

$$W_7 = 0.00480 \cdot \frac{P \cdot l_p^2}{E_b \cdot I_0}; \quad (8)$$

$$W_8 = 0.00066 \cdot \frac{P \cdot l_p^2}{E_b \cdot I_0}; \quad (9)$$

$$W_9 = 0.00146 \cdot \frac{P \cdot l_p^2}{E_b \cdot I_0}; \quad (10)$$

$$W_{10} = 0.00041 \cdot \frac{P \cdot l_p^2}{E_b \cdot I_0}. \quad (11)$$

Plotting the diagram of the fictitious moments from the action of the weights W_i is not difficult. The diagram M in our case is a broken line. In places where the diagram is broken (q_f), i.e., in sections 2 ÷ 6, the fictitious moments M coincide with the deflections in these sections. The control deflection f_c under the load P, shown in the M diagram (see Fig. 4e), is numerically equal to 19.9 mm.

Falsone (2018) gives an explanation for the modern assumption of a concentrated external moment, interpreted as a generalized function (doublet), and shear deformation, which determines the contradictory discontinuities in deflection laws.

Thus, with the control load for stiffness P_c = 178 kN, the control deflection at a given load is assumed to be f_c = 19.9 mm.

Results and Discussion

The values of the control loads, the control deflection, and the control crack opening width for testing the UPB 185.25 unit for stiffness, crack resistance, and strength, according to the calculation results, were taken as follows:

1) by stiffness — P_c = 178 kN;
2) by crack resistance — P_c = 410 kN;
3) by strength — P_c = 887 kN;
4) by deflection — f_c = 19.9 mm;
5) by crack opening — a_{cr} = 0.2 mm.

The experimental value of the UPB 185.25 unit deflection in tests under the action of the control load for stiffness P_c = 178 kN in accordance with Clause 9.2.4 of GOST 8829-94 when testing one product should not exceed the control value of the deflection by more than 10 %.

The experimental crack opening width in tests under the action of the control crack resistance load P_c = 410 kN in accordance with Clause 9.3.4 of GOST 8829-94 when testing one product should not exceed the control crack opening width multiplied by a factor of 1.05.

Fig. 5 shows a diagram with the layout of deflectometers along the length of the unit and the outline of the deflections of the UPB 185.25 unit along its length during testing

The analysis of the UPB 185.25 unit deflection outline along the unit length (Fig. 5) shows that the deflections in the right part of the UPB 185.25 unit deflection outline have larger values compared to the deflections in the left part. This outline of the deflections is quite natural since the right side of the unit is less stiff compared to its left side.

Fig. 6 shows a diagram of deflections in the middle section of the UPB 185.25 unit under the load P. The analysis of the deflection diagram allows us to note the following.

At the first stage of testing, the stiffness of the unit was evaluated. With the control load for stiffness P_c = 178 kN, the experimental deflection of the unit should not exceed the control value f_c = 19.9 mm. Upon reaching this load, the experimental deflection in the considered section of the unit had a value equal to f_{exp} = 18.3 mm, which was 92% of the control deflection.

At the second stage of testing, the crack resistance of the unit was evaluated. With the control load for crack resistance P_c = 410 kN, the experimental crack opening width should not exceed the control value a_{cr} = 0.2 mm. At the experimental load P_{exp} = 410 kN, the crack opening width in the beam concrete was a_{exp} = 0.15 mm.

At the third (last) stage of testing, the strength of the unit was evaluated. The control load when testing the strength of the unit with the safety factor of C = 1.3 was P_c = 887 kN. During the control tests, the experimental load P_{exp} = 910 kN was achieved, which amounted to 108 %. When the experimental load P_{max} = 910 kN was reached, the maximum output of the hydraulic jack plunger was achieved, and in this regard, further loading was suspended. The nature of the increase in the deflections and the assessment of the stress-strain state of the UPB 185.25 unit showed that the limit state was

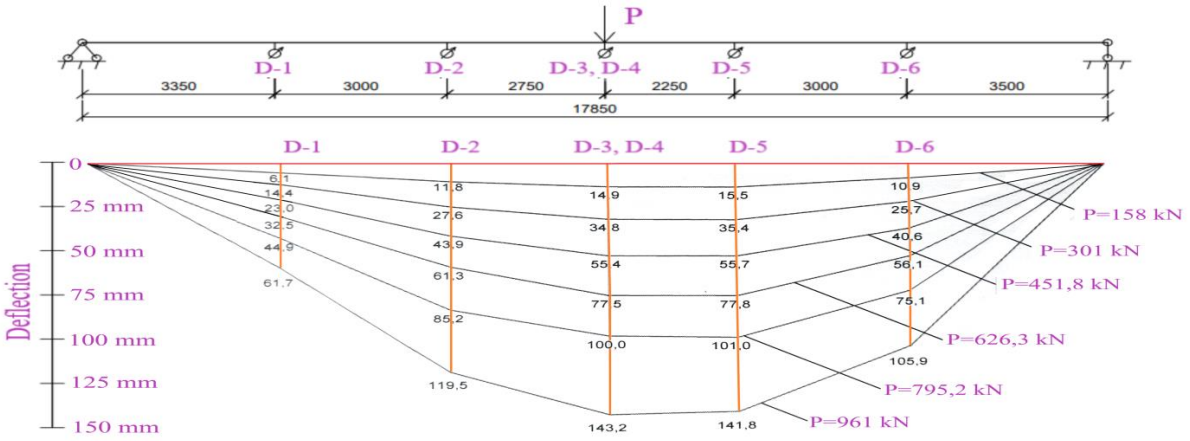

Fig. 5. Diagram with the layout of deflectometers along the length of the unit and the outline of the deflections of the UPB 185.25 unit along its length during testing

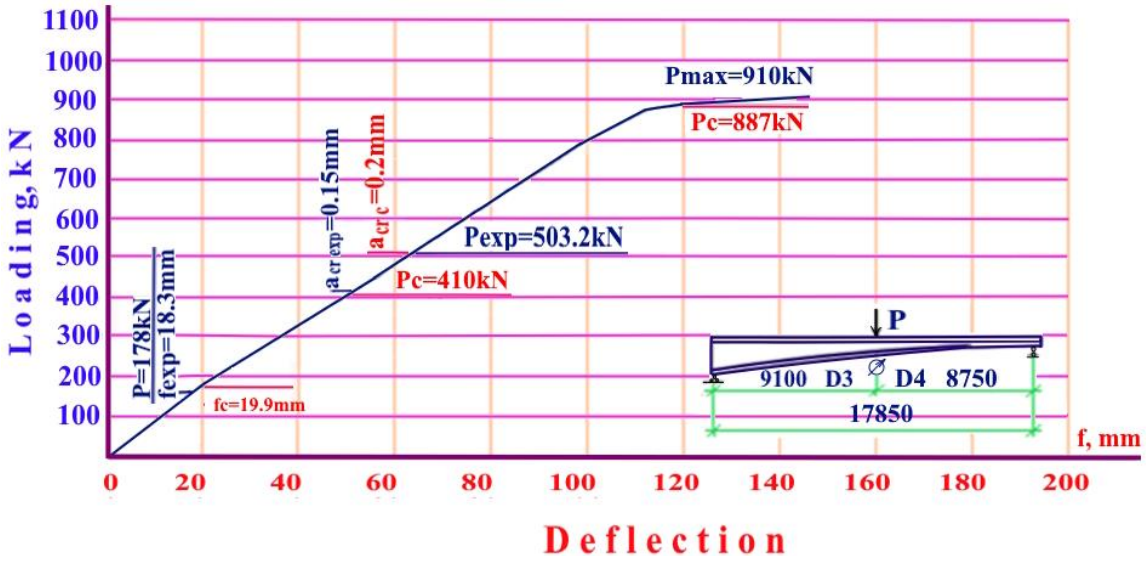

Fig. 6. Diagram of deflections in the middle section of the UPB 185.25 unit

not reached, and it had reserves in terms of bearing capacity.

Thus, the breakdown of the conical beam into separate blocks of variable cross-section confirmed the correctness of the chosen design strategy. Zheng and Ji (2011) showed that equivalent representations of beams with periodically variable cross-section in the form of several steps of variable cross-section give good convergence in calculating the displacements and the fundamental natural frequency of the beams.

4 Spatial model of the UPB unit built in MIDAS FEA NX

Three-dimensional computational modeling of a reinforced concrete beam by the finite element method was performed in MIDAS FEA NX. Fig. 7 shows a spatial model of the UPB unit built in MIDAS FEA NX. Fig. 8 shows a general view of the UPB unit reinforcement, and Fig. 9 shows a grid scheme adopted for the UPB unit 185.25.

At the first stage, the calculation of the beam and its modeling with the help of rod elements were performed.

The following parameters were used:

- element type — bending beam element;
- load type — uniaxial bending;
- maximum reinforcement percentage — 10%.

Longitudinal reinforcement consisting of A400 class rebars and transverse reinforcement consisting of A240 class rebars were taken into account in the calculation. Fig. 8 shows the adopted data for the reinforcing bars.

For concrete, the parameters specified in Figs. 10, 11 were used. In this case, the accepted diagrams of concrete deformation in tension and compression for concrete class B40 are taken for non-linear calculation at short-term loading at moisture content 40–75% according to Clause 6.1.20 of SP 63.13330.2018 “Concrete and reinforced concrete structures”. Three-dimensional solid finite elements

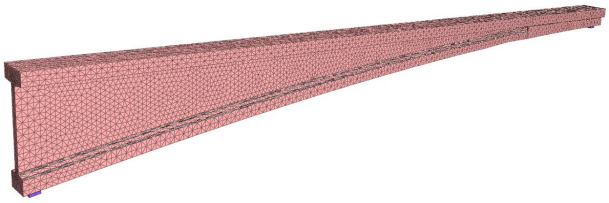

Fig. 7. Spatial model of the UPB 185.25 unit built in MIDAS FEA NX

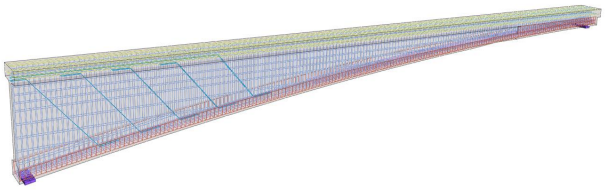

Fig. 8. General view of the UPB 185.25 unit reinforcement

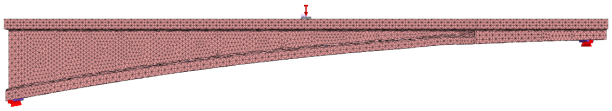

Fig. 9. Grid scheme of the UPB 185.25 unit

are used for concrete and three-dimensional beam elements are used for reinforcement.

According to the calculation at a vertical concentrated load of 888.85 kN, vertical displacement is 142.5 mm (Fig. 12).

The plastic stage of the reinforcement, the patterns of maximum longitudinal forces and maximum stresses in the reinforcement (Fig. 13) practically coincide with the theoretical equations for the strength of materials.

In addition, the calculation of the 3D model of the beam with cracking was performed. The crack dimensions were set in the tensile zone based on the initial calculation data.

Then the crack resistance of the beam was calculated. By iteration and compliance with the above conditions, the maximum value of crack opening equal to 0.226 mm was obtained (Fig. 14).

The maximum value of the crack opening width of 0.226 mm is significantly higher than the experimental value, which is apparently due to the failure to consider the behavior of the inclined reinforcement at the plastic stage.

Fig. 15 shows a comparative diagram of the deflections in the middle section.

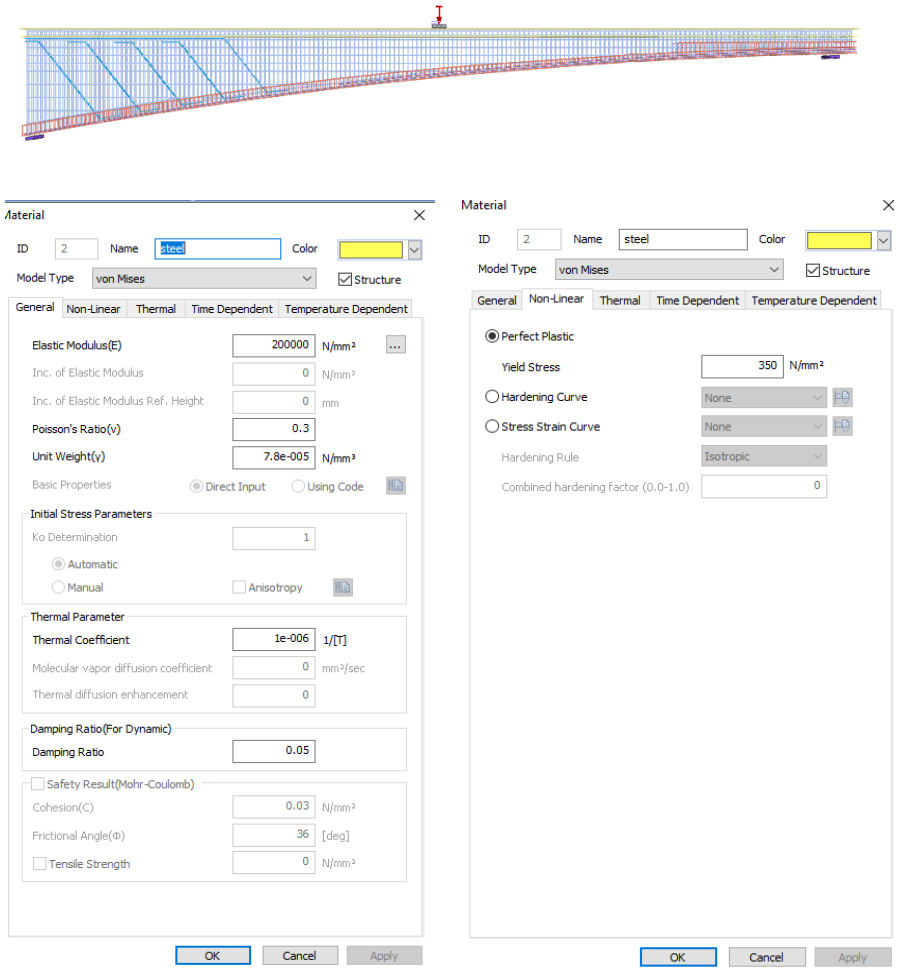

Fig. 10. Adopted data for rebars

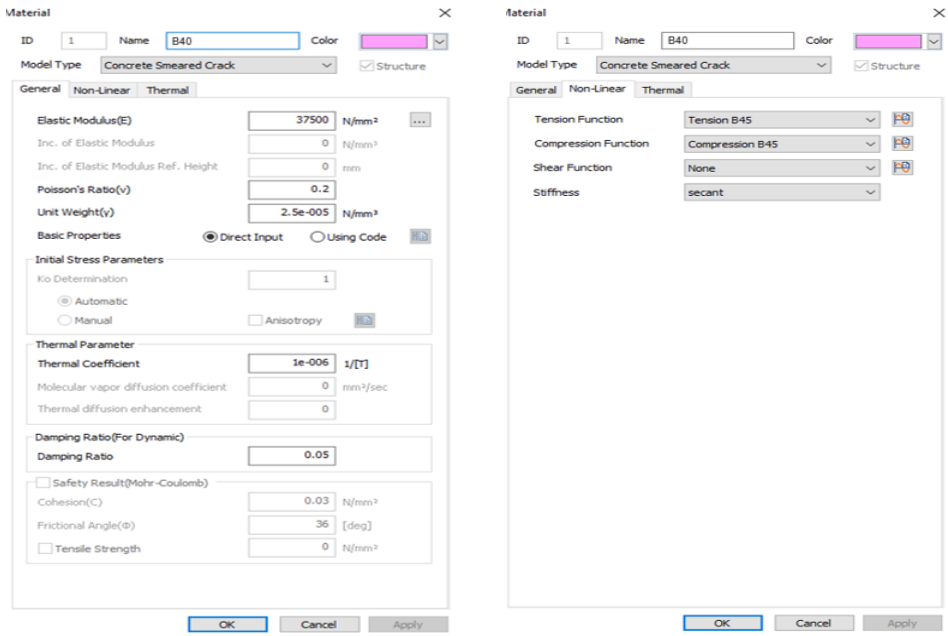

Fig. 11. Adopted data for concrete

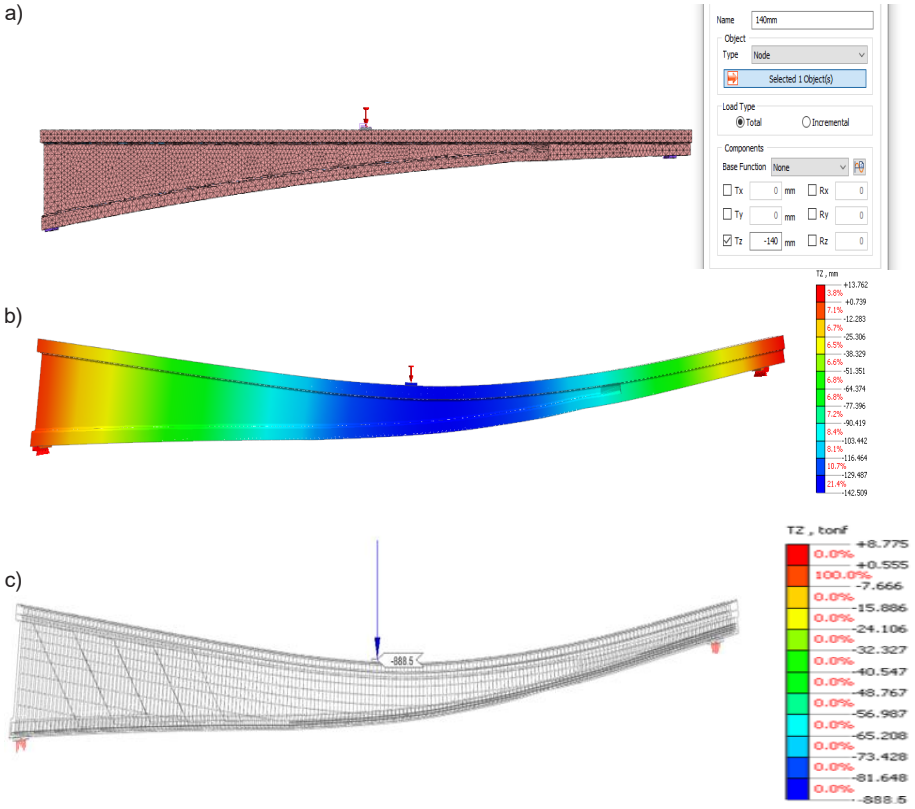

Fig. 12. Results of the beam calculation for maximum deflections: *a — deflection of 140 mm; b — maximum beam deflection of 142.5 mm; c — maximum load of 888.5 kN*

In addition, the maximum deflections were calculated for different classes of concrete. Fig. 16 shows a comparative diagram of the deflections for different concrete classes.

If for concrete of class B40, the maximum design load P_{max} = 888.5 kN practically coincided with the expected P_c = 887 kN, then for concretes of classes B35 and B25, there is a decrease in strength by 2.36 % and 6.7 %, respectively.

Experimental confirmation is necessary to substantiate the possibility of using concrete of class B35 in these products. The use of concrete of class B25 in these

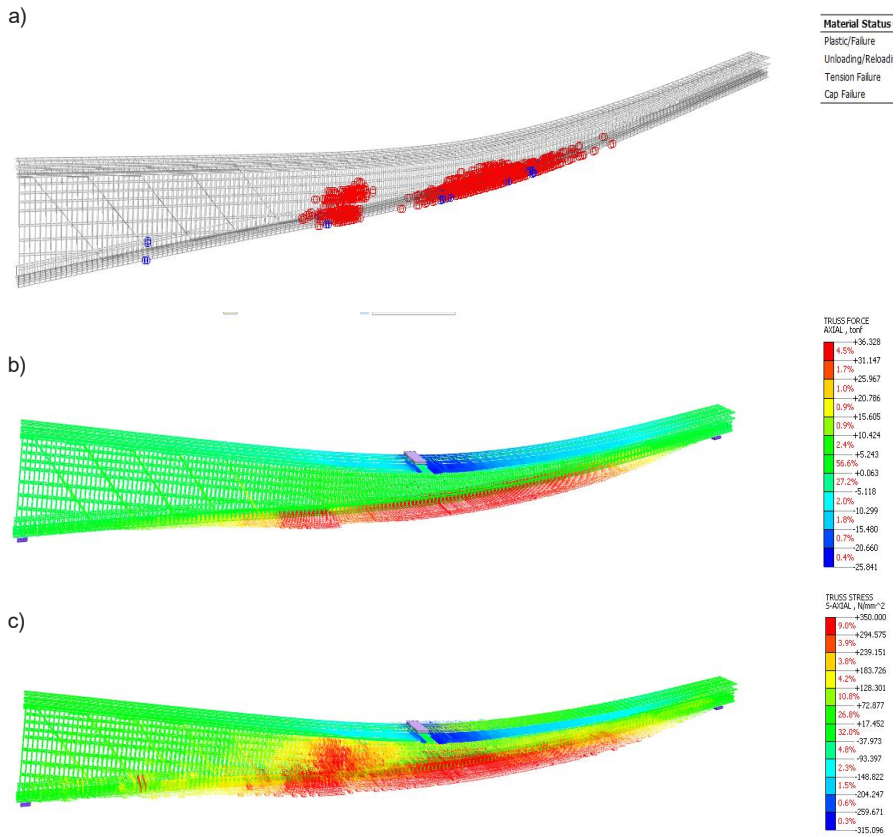

Fig. 13. Maximum deformations and stresses in the reinforcement at the limit stage: *a — "plastic status" in the UPB unit rebars; b — maximum longitudinal forces in the UPB unit rebars; c — maximum stresses in the UPB unit rebars*

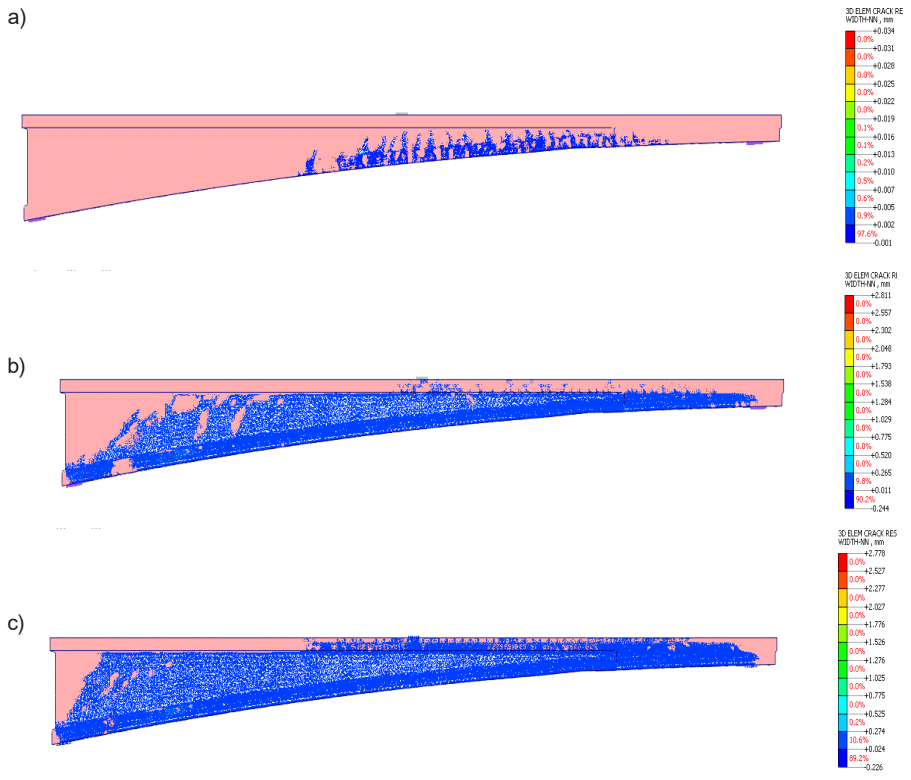

Fig. 14. Crack propagation in the concrete block: *a — at 0.05*140 mm pitch (5 % of the specified displacement); at 0.4*140 mm pitch (40% of the specified displacement); at 1.0*140 mm pitch (100 % of the specified displacement)*

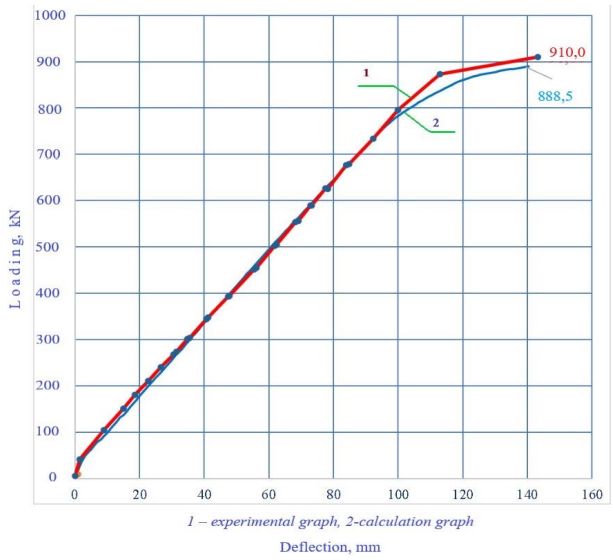

Fig. 15. Diagram of deflections in the middle of the UPB unit

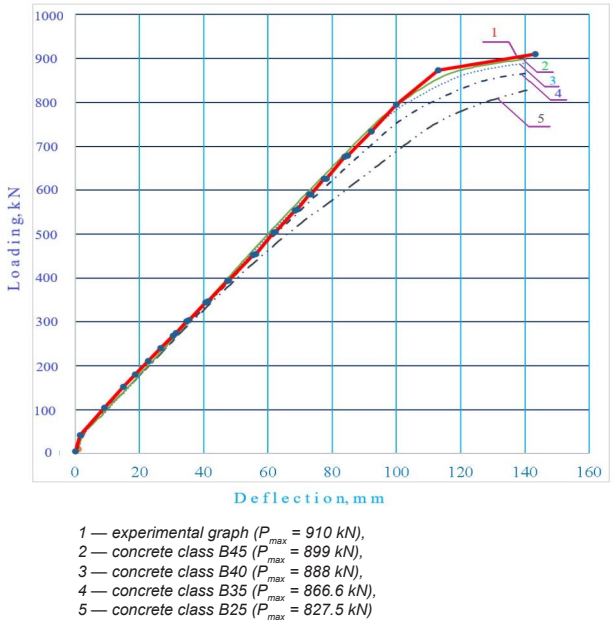

Fig. 16. Diagram of deflections in the middle of the UPB unit for different classes of concrete

products is considered inexpedient due to a decrease in strength by 6.7 % in comparison with the reference beam and the absence of prestressed reinforcement.

Conclusions

• The control load for the UPB 185.25 unit stiffness testing was P_c = 178 kN, and the control deflection was taken equal to f_c = 19.9 mm. Upon reaching the experimental load equal to P_{exp} = 178 kN, the experimental deflection had a value equal to f_{exp} = 18.3 mm, which was 92% of the control deflection. In terms of stiffness, the UPB 185.25 unit meets the requirements of GOST 8829-94 and SP RK 3.03-112-2013.

• The control load for the UPB 185.25 unit crack resistance testing was P_c = 410 kN, and the control crack opening width was taken equal to a_{cr} = 0.2 mm. At the experimental load P_{exp} = 410 kN, the crack opening width in the beam concrete was a_{exp} = 0.15 mm. Only when the experimental load equal to the value of P_{exp} = 503.2 kN was reached, the experimental crack opening width was a_{exp} = 0.2 mm. In terms of crack resistance, the UPB 185.25 unit meets the requirements of GOST 8829-94 and SP RK 3.03-112-2013.

• The control load for the UPB 185.25 unit according to the strength test was P_c = 887 kN. In the tests, the experimental load equal to the value of P_{exp} = 910 kN was achieved. The nature of the increase in the deflections and the assessment of the stress-strain state of the experimental product showed that, at a given test load, the UPB 185.25 unit had reserves in terms of its bearing capacity. In terms of strength, the UPB 185.25 unit meets the requirements of GOST 8829-94 and SP RK 3.03-112-2013.

• The results of beam calculation in Midas FEA NX showed high convergence of the design (888.5 kN) and experimental load (887 kN) in terms of beam strength for concrete class B40.

The results of the beam calculation with concrete of B35 and B25 classes showed that it is inexpedient to use concrete of B25 class due to a decrease in strength by 6.7% in comparison with the reference beam and the absence of prestressed reinforcement.

References

Balduzzi, G., Aminbaghai, M., Sacco, E., Füssl, J., Eberhardsteiner, J., and Auricchio, F. (2016). Non-prismatic beams: A simple and effective Timoshenko-like model. *International Journal of Solids and Structures*, Vol. 90, pp. 236–250. DOI: 10.1016/j.ijsolstr.2016.02.017.

Barham, W. S. and Idris, A. A. (2021). Flexibility-based large increment method for nonlinear analysis of Timoshenko beam structures controlled by a bilinear material model. *Structures*, Vol. 30, pp. 678–691. DOI: 10.1016/j.istruc.2021.01.023.

Cazzani, A., Malagù, M., and Turco, E. (2016). Isogeometric analysis of plane-curved beams. *Mathematics and Mechanics of Solids*, Vol. 21, Issue 5, pp. 562–577. DOI: 10.1177/1081286514531265.

Chockalingam, S. N., Nithyadharan, M., and Pandurangan, V. (2020). Shear stress distribution in tapered I-beams: Analytical expression and finite element validation. *Thin-Walled Structures*, Vol. 157, 107152. DOI: 10.1016/j.tws.2020.107152.

Chockalingam, S. N., Pandurangan, V., and Nithyadharan, M. (2021). Timoshenko beam formulation for in-plane behaviour of tapered monosymmetric I-beams: Analytical solution and exact stiffness matrix. *Thin-Walled Structures*, Vol. 162, 107604. DOI: 10.1016/j.tws.2021.107604.

Committee for Construction, Housing and Communal Services and Land Management of the Ministry of National Economy of the Republic of Kazakhstan (2015). *Regulations SP RK 3.03-112-2013. Bridges and culverts*. Astana: Ministry of National Economy of the Republic of Kazakhstan, 717 p.

Falsone, G. (2018). The use of generalized functions modeling the concentrated loads on Timoshenko beams. *Structural Engineering and Mechanics,* Vol. 67, No. 4, pp. 385–390. DOI: 10.12989/sem.2018.67.4.385.

Gosstroy of Russia (1998). *State Standard GOST 8829-94. Reinforced concrete and prefabricated concrete building products. Loading test methods. Assessment of strength, rigidity and crack resistance*. Moscow: Gosstroy of Russia, 27 p.

Government of the Republic of Kazakhstan (2010). *Technical Regulations "Safety requirements for buildings and structures, building materials and products".* Astana: Government of the Republic of Kazakhstan, 40p.

Gusev, B. V. and Saurin, V. V. (2017). *On vibrations of inhomogeneous beams*. [online]. Available at: http://www.info-rae.ru/o-kolebaniyax-neodnorodnyx-balok/ [Date accessed March 1, 2023].

Gusev, B. V. and Saurin, V. V. (2018). Variational approaches to finding eigenvalues for beams with variable cross-section. *Innovations and Investments*, No. 3, pp. 253–264.

Jalairov, A., Kumar, D., Kassymkanova, K.-K., Nuruldaeva, G., Imankulova, A. (2022a). Structural behavior of prestressed concrete bridge girder with monolithic joint. Communications - Scientific Letters of the University of Zilina, Vol. 24, Issue 4, pp. D150–D159. DOI: 10.26552/com.C.2022.4.D150-D159.

Petukhov, L. V. (1980). Thin curvilinear beams of minimum weight. *Journal of Applied Mathematics and Mechanics*, Vol. 44, Issue 4, pp. 508–512. DOI: 10.1016/0021-8928(80)90042-8.

Jalairov, A., Kumar, D., Kassymkanova, K.-K., Sarsembekova, Z., Nuruldaeva, G., and Jangulova, G. (2022b). Structural behavior of prestressed concrete bridge girder with epoxy joint. *Communications - Scientific Letters of the University of Zilina*, Vol. 24, Issue 2, pp. D59–D71. DOI: 10.26552/com.C.2022.2.D59-D71.

Ministry of Construction, Housing and Utilities of the Russian Federation (2019). *Regulations SP.63.13330.2018. Concrete and reinforced concrete structures. General provisions.* Moscow: Standartinform, 117 p.

Resan, S. F. and Zamel, J. K. (2021a). Flexural behavior of developed reinforced concrete beams of non prismatic flanges. *Materials Today: Proceedings*, Vol. 42, Part 5, pp. 2974–2983. DOI: 10.1016/j.matpr.2020.12.808.

Resan, S. F. and Zamel, J. K. (2021b). Rotation capacity assessment in developed non prismatic flanged reinforced concrete Tee beams. *Case Studies in Construction Materials*, Vol. 14, e00517. DOI: 10.1016/j.cscm.2021.e00517.

Ruditsyn, M. N. (1940). *Calculation of beams with variable cross-section, framed and strutted systems by breaking loads*. [online] Available at: https://elib.belstu.by/bitstream/123456789/35163/1/%D0%A0%D1%83%D0%B4%D0%B8%D1%86%D1%8B%D0%BD.pdf [Date accessed March 1, 2023].

Saurin, V. V. (2019). Analysis of dynamic behavior of beams with variable cross-section. *Lobachevskii Journal of Mathematics*, Vol. 40, Issue 3, pp. 364–374. DOI: 10.1134/S1995080219030168.

Shalkarov, A. A., Karasay, S. Sh., Tanirbergenov, A. K., and Murzalina, G. B. (2018). Monitoring the manufacture of UBS 185.14 blocks for the overhead span structure in Almaty. *Bulletin of Omsk regional Institute*, No. 4, pp. 13–26.

Smirnov, A. F. (ed.). (1961). *Strength of materials*. Moscow: Transjeldorızdat, 591 p.

Tayfur, Y., Darby, A., Ibell, T., Orr, J., and Evernden, M. (2019). Serviceability of non-prismatic concrete beams: Combined-interaction method. *Engineering Structures,* Vol. 191, pp. 766–774. DOI: 10.1016/j.engstruct.2019.04.044.

Timoshenko, S. P. (1965). Strength of materials. Part 1. Elementary Theory and Problems. Moscow: Nauka, 363 p.

Wang, C. M., Thevendran, V., Teo, K. L., and Kitipornchai, S. (1986). Optimal design of tapered beams for maximum buckling strength. *Engineering Structures*, Vol. 8, Issue 4, pp. 276–284. DOI: 10.1016/0141-0296(86)90035-0.

Yassopoulos, C., Leake, C., Reddy, J. N., and Mortari, D. (2021). Analysis of Timoshenko–Ehrenfest beam problems using the Theory of Functional Connections. *Engineering Analysis with Boundary Elements*, Vol. 132, pp. 271–280. DOI: 10.1016/j.enganabound.2021.07.011.

Zheng, T. and Ji, T. (2011). Equivalent representations of beams with periodically variable cross-sections. *Engineering Structures*, Vol. 33, Issue 3, pp. 706–719. DOI: 10.1016/j.engstruct.2010.11.007.

Zhernakov, V. S., Pavlov, V. P., and Kudoyarova, V. M. (2017). Spline-method for numerical calculation of natural-vibration frequency of beam with variable cross-section. *Procedia Engineering*, *Vol. 206*, pp. 710–715. DOI: 10.1016/j.proeng.2017.10.542.

Zhong, J., Zhuang, H., Shiyang, P., and Zhou, M. (2021). Experimental and numerical analysis of crack propagation in reinforced concrete structures using a three-phase concrete model. *Structures,* Vol. 33, pp. 1705–1714. DOI: 10.1016/j.istruc.2021.05.062.

Zhou, M., Fu, H., Su, X., and An, L. (2019a). Shear performance analysis of a tapered beam with trapezoidally corrugated steel webs considering the Resal effect. *Engineering Structures*, Vol. 196, 109295. DOI: 10.1016/j.engstruct.2019.109295.

Zhou, M., Liao, J., Zhong, J., An, L., and Wang, H. (2021). Unified calculation formula for predicting the shear stresses in prismatic and non-prismatic beams with corrugated steel web. *Structures*, Vol. 29, pp. 507–518. DOI: 10.1016/j.istruc.2020.11.060.

Zhou, M., Shang, X., Hassanein, M. F., and Zhou, L. (2019b). The differences in the mechanical performance of prismatic and non-prismatic beams with corrugated steel webs: A comparative research. *Thin-Walled Structures*, Vol. 141, pp. 402–410. DOI: 10.1016/j.tws.2019.04.049.

РАСЧЕТ И ИСПЫТАНИЯ УСИЛЕННОЙ КОНИЧЕСКОЙ МОСТОВОЙ БАЛКИ

Асылхан Джалаиров (Assylkhan Jalairov)[1], Даурен Кумар (Dauren Kumar)[2]*,
Нуржан Досаев (Nurzhan Dosaev)[3], Гульжан Нурулдаева (Gulzhan Nuruldaeva)[4],
Хайни-Камаль Касымканова (Khaini-Kamal Kassymkanova)[4],
Гульшат Мурзалина (Gulshat Murzalina)[4]

[1]Кафедра «Транспортное строительство, мосты и тоннели», Международный транспортно-гуманитарный университет, Алматы, Республика Казахстан

[2]Кафедра картографии и геоинформатики, Казахский национальный университет имени Аль-Фараби, Алматы, Республика Казахстан

[3]Департамент науки и внедрения новых технологий, Национальный центр качества дорожных активов, Астана, Республика Казахстан

[4]Университет им. К. И. Сатпаева, Алматы, Республика Казахстан

*E-mail: daurendkb@gmail.com

Аннотация
Введение: в статье рассматривается соответствие фактических прочностных и деформативных свойств унифицированного сборного блока (далее — УСБ 185.25) расчетным данным. **Цель исследования** заключалась в проверке сходимости экспериментальных данных по железобетонной балке с переменным контуром нижнего пояса и расчетных допущений. **Методы:** В ходе исследования моменты инерции на каждом участке блока брались усредненными, пошагово. Каждый участок рассчитывался отдельно. Затем результаты суммировались. Кроме того, расчетные значения были проверены с помощью метода конечных элементов в MIDAS. **Результаты:** Принятые расчетные допущения, основанные на результатах испытаний, показали высокую сходимость результатов и подтвердили соответствие балки по жесткости, трещиностойкости и прочности. Контрольная ширина раскрытия трещин a_{cr} = 0,2 мм была достигнута при нагрузке 503,2 кг, что на 22,7% выше расчетной нагрузки.

Ключевые слова: прогиб балки, контрольные нагрузки, трещиностойкость, графоаналитический метод, УСБ 185, анализ МКЭ.